ANNALES SOCIETATIS GEOLOGORUM POLONIAE
ROCZNIK POLSKIEGO TOWARZYSTWA GEOLOGICZNEGO
v. 51—3/4: 339—352 Kraków 1981

Krzysztof P. KRAJEWSKI

PHOSPHATE PIZOLITE STRUCTURES FROM CONDENSED LIMESTONES OF THE HIGH-TATRIC ALBIAN (TATRA MTS)

(Pl. I—V and 2 Figs.)

Fosforanowe formy pizolitowe ze skondensowanych wapieni albu wierchowego (Tatry)

(Pl. I—V i 2 fig.)

Krzysztof P. Krajewski: Phosphate pizolite structures from condensed limestones of the high-tatric Albian (Tatra Mts) Ann. Soc. Geol. Poloniae, 51—3/4: 339—352.

Abstract. Phosphate pizolite structures occur at hardground surfaces in the high-tatric Albian condensed limestones (Tatra Mts). Their origin is due to accretional growth and intraformational reworking. They were slowly growing by accretion of colloidal phosphates, in form of a homogeneus mass with some microglobules (supposedly phosphate-enriched microorganisms), and non-phosphatic detritic material. The accretion was proceeding spherically or hemispherically because of the intraformational reworking. The phosphate pizolite structures developed under conditions of periodically reworked hardground. The present-day mineral composition of these structures is due to diagenetic processes, namely a crystallization of carbonate fluorapatite related to an activation of organic matter.

Key words: phosphate pizolite structures, hardgrounds, Albian, Tatra Mts, Poland

Krzysztof P. Krajewski: Instytut Nauk Geologicznych PAN, al. Żwirki i Wigury 93 02-089 Warszawa

manuscript received: November 1980 accepted: February 1981

Treść: Opisane zostały fosforanowe formy pizolitowe (fig. 1—2) występujące na powierzchniach twardych den w skondensowanych wapieniach albu wierchowego w Tatrach Polskich. Dokładne badania w mikroskopie polaryzacyjnym i w mikroskopie skaningowym (pl. I—V) oraz analizy rentgenostrukturalne (tabl. 1) wykazały, że są one zbudowane z węglanowego fluoroapatytu (1,3% CO_2). Wszystkie obserwowane apatyty są diagenetyczne, występujące w różnych stadiach rekrystalizacji z pierwotnej żelopodobnej substancji fosforanowej. Powolny wzrost pizolitów wynikał z akrecji koloidalnych fosforanów, jako homogenicznej masy i mikro-

globul (wzbogaconych w fosforany mikroorganizmów). Rekrystalizacja żelopodobnych fosforanów związana była z diagenetycznym uruchamianiem materii organicznej. Aktywność prądowa, w środowisku twardego dna morskiego, powodowała przeróbkę badanych struktur oraz akrecję niefosforanowego materiału detrytycznego. Specyficzny stosunek pomiędzy akrecyjnym wzrostem i przeróbką doprowadził do powstania sferycznych do półsferycznych form pizolitowych.

INTRODUCTION

The investigated material was derived from condensed phosphatic and glauconitic limestones of the high-tatric Albian of the Polish Tatra Mts. These limestones form a thin lithologic set overlying thick reefal Urgonian limestones and underlying, in turn, deep-water marls of the uppermost Albian to Cenomanian (Passendorfer, 1921, 1930; Kušik, 1959; Turnau-Morawska, 1960; Niegodzisz, 1965; Lefeld, 1968). They are considered to be deposited under open-shelf conditions (Kotański, 1961; Borza and Martiny, 1962).

The high-tatric Albian limestones include several hardground surfaces. These surfaces are strongly mineralized and bear much evidence for intraformational reworking. They are, indeed, associated with abundant phosphoclasts, abraded and mineralized fossil remains, and mineral stromatolites and oncolites. The clasts overlying the hardgrounds include also infrequent phosphate pizolite structures.

DESCRIPTION

General remarks. The investigated phosphate pizolite structures consist of phosphate-pizolitic laminae and non-phosphatic detritic material. They are highly variable in shape and range up to 2 cm in diameter. The former ones (fig. 1) show a small nucleus covered with a thick, concentrically laminated phosphatic coating. The others (fig. 2) always are attached to larger clasts.

All these pizolite structures include detritic material stabilized by phosphatic laminae (pl. I, fig. 2). The detritic material includes carbonate pellets, quartz grains, planktic forams, calcisphaeres, crinoid fragments, and other skeletal grains. These clasts occur in the form of detritic lenses within pizolitic lamination. The proportion of detritic material is highly variable but it may considerably prevail over phosphate-pizolitic laminae.

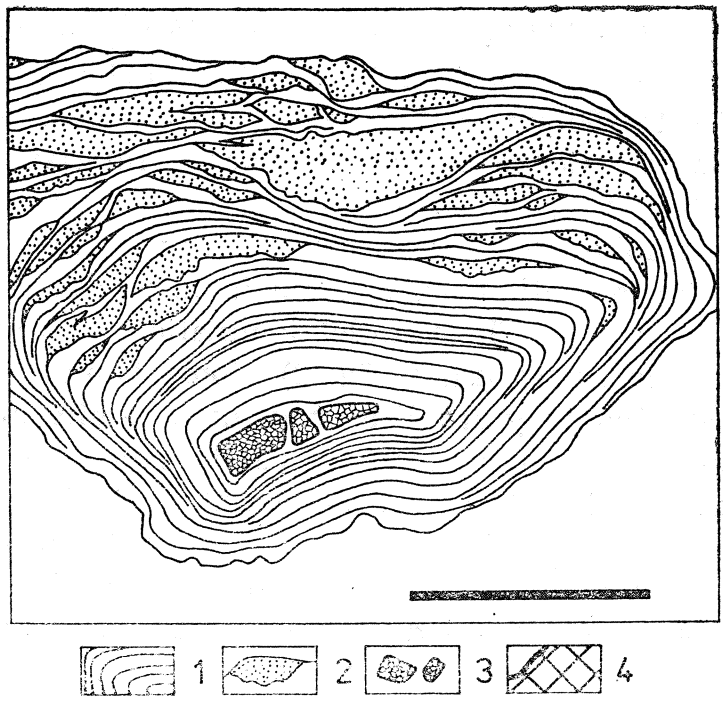

Fig. 1. Phosphate pizolite structure; drawing after a thin section. Note the asymmetry caused by accretion of non-phosphatic detritic material. 1 — phosphate-pizolite lamination; 2 — lenses of non-phosphatic detritic material; 3 — larger-sized calcareous skeletal fragments; 4 — phosphoclast; bar equals 5 mm

Fig. 1. Fosforanowa forma pizolitowa; rysunek z płytki cienkiej. Wyraźna asymetryczność spowodowana akreacją niefosforanowego materiału detrytycznego. 1 — fosforanowa laminacja pizolitowa; 2 — soczewki niefosforanowego materiału detrytycznego; 3 — większe kalcytowe fragmenty szkieletowe; 4 — fosfoklast; skala odpowiada 5 mm

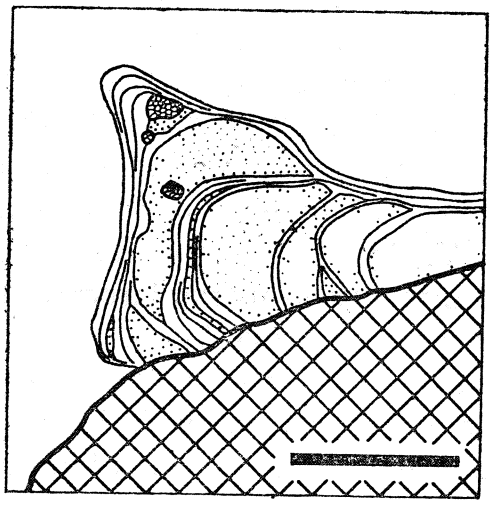

Fig. 2. Phosphate semi-pizolite structure developed at a large-sized phosphoclast; drawing after a thin section. Bar equals 2.5 mm; for other explanations see fig. 1

Fig. 2. Fosforanowa forma pół-pizolitowa rozwinięta na dużym fosfoklaście; rysunek z płytki cienkiej. Skala odpowiada 2.5 mm; pozostałe objaśnienia na fig. 1

Phosphate-pizolitic laminae. The phosphate-pizolitic laminae are more or less constant in structure and texture (pl. I, fig.1), ranging from 80 to 400 μm in thickness. They consist of collophane with minor amounts of micrite and microsparite. Interlaminar boundaries are accentuated by thin (up to a few μm) films of iron oxides, or textural changes in collophane, or an increased proportion of organic matter. The laminae are continuous, constant in thickness, regularly parallel to each other as a rule. The parallel lamination, however, may be disturbed by detritic lenses (pl. I, fig. 2). Some laminae consist of very fine microsparite, but they are discontinuous, laterally intergrading with phosphatic laminae. Other laminae are partly composed of microcrystalline apatite (pl. V, figs 1—2). As evidenced by SEM observations, the laminae show irregular surfaces, with microgranular ups and downs (pl. III, figs 1—2). These surfaces are built up by aggregates of ultramicrocrystalline phosphates associated here and there with massive phosphates.

Intralaminar microstructure. The phosphatic laminae show microglobular structure (pl. II, figs 1—2; pl. III, figs 3—4). They consist of microglobules (5 to 30 μm in diameter) embedded within collophane matrix. The pizolite structures are highly variable in density of microglobules; in fact, there are structures with microglobules being virtually absent from some parts. The microglobules show plastic deformations at their mutual contacts (pl. II, fig. 2). Infrequently, they are homogeneous, dark, and isotropic. Most commonly, they include aggregates of ultra- and/or microcrystalline phosphates inside (pl. III, figs. 5—6), covered with a dark and isotropic coating. The microglobules are cemented with collophane which is microlaminated or less commonly homogeneous. The microlamination is consistent with the pizolitic lamination. It is expressed by an alternation of dark and light collophane microlaminae (this variation in colour reflecting a variation in content of organic matter) ranging from 3 to 6 μm in thickness (pl. II, fig. 2). The microlaminae never cut across microglobular boundaries. At a contact with detritic material, the underlying collophane microlaminae show load deformations (pl. IV, figs 1—2). As evidenced by SEM observations, the collophane most commonly is ultramicrocrystalline and only subordinately massive in nature (pl. V, figs 3—4).

The pizolitic laminae include also variable amounts of non-detritic carbonates, micrite and microsparite, in form a small enclaves cutting discordantly across the collophane microlaminae as well as the microglobules.

Microfossil fills. The detritic material within the phosphate--pizolitic lamination commonly includes planktic foraminiferal tests and calcisphaeres (pl. IV, figs. 3—4). These microfossils are filled up with massive phosphates developed from the margins of a chamber inwards;

Table 1
Tabela 1

XRD data of carbonate fluorapatite from the phosphate pizolite structures (CuKα radiation)
Dane rentgenograficzne węglanowego fluoroapatytu z fosforanowych form pizolitowych (promieniowanie CuKα)

Examined sample Badana próbka			Standard after ASTM Wzorzec według ASTM Fluorapatite $Ca_5(PO_4)_3F$ Fluoroapatyt	
d(Å)	I		d(Å)	I
8.05	0.5		8.12	8
5.25	0.5		5.25	4
			4.684	< 1
4.040	0.5		4.055	8
			3.872	8
			3.494	< 1
3.445	4.5		3.442	40
3.165	1.5		3.167	14
3.055	1.5		3.067	18
2.797	10		2.800	100
2.778	6		2.772	55
2.669	5		2.702	60
2.624	2.5		2.624	30
2.508	0.5		2.517	6
2.285	0.5		2.289	8
2.244	2		2.250	20
			2.218	4
2.136	0.5		2.140	6
			2.128	4
2.060	0.5		2.061	6
			2.028	2
			1.997	4
1.935	2.5		1.937	25
1.882	1.5		1.884	14
			1.862	4
1.837	3		1.837	30
1.794	1		1.797	16
1.768	1	(410)	1.771	14
1.745	1		1.748	14
1.721	1.5	(004)	1.722	16
			1.684	< 1
1.636	0.5		1.637	6
1.608	0.5		1.607	4
			1.580	2
			1.562	< 1
			1.534	6
			1.524	4
			1.501	4
			1.497	4
1.467	1		1.468	8

however, the center commonly remains void. The fills are at variable stages of recrystallization of massive phosphates, up to ultra- and/or microcrystalline ones.

XRD analysis (under CuKα radiation) demonstrates that the crystalline phosphate phase of the pizolite structures represents the carbonate fluorapatite (table 1). As indicated by dispersion of the (004) and (410) reflexes (cf. Gulbrandsen, 1970), the proportion of carbon dioxide in the apatite lattice amounts to 1.3%.

DISCUSSION

Phosphates abound in the condensed high-tatric Albian limestones of the Tatra Mts but nonetheless, phosphate pizolite structures occur there only infrequently. In fact, the majority of phosphates in this lithologic set displays replacement structures in hardgrounds, phosphoclasts, and mineral stromatolites, while the phosphate pizolite structures show no evidence for replacement origin of the phosphate matter. The microstructure and the absence of any carbonate relics are suggestive of the primary nature of the phosphates in the pizolites. The primary nature of phosphates, however, is not equivalent to the primary nature of the apatite. To the contrary, the occurence of massive, ultra-, and microcrystalline phosphate aggregates at variable stage of recrystallization is indicative of deposition of gel-like phosphate matter than of direct chemical precipitation of apatite from sea-water. The surfaces of laminae of the investigated pizolite structures strikingly resamble those observed in present-day accretional phosphatic pellets (Birch, 1979b). Colloidal accretion of phosphates is still insufficiently documented but this process was invoked to explain formation of phosphate ooids in the Californian shelf (Dietz et al., 1942; Emery, 1960). Furthermore, laminated phosphates and coatings developed on phosphorite nodules, resambling very closely in structure the phosphate pizolites investigated herein, were described from the Miami Terrace and interpreted as an effect of deposition of amorphous collophane (Mullins and Neumann, 1979). This is also the case with phosphate structures observed in the Ebon atoll, Micronesia (Veeh and Burnett, 1978). One may also recall concretional, oolitic and pelletal phosphorites from the South and West African shelf which include poorly crystalline phosphates (Fuller, 1979, and references therein). In fact, direct chemical precipitation of apatite from sea-water has been demonstrated to be theoretically possible (Gulbrandsen, 1969; Berge, 1972; Nathan and Lucas, 1976), but practical feasibility of this process may nevertheless be questionable (McConnell, 1965, 1973;

Pevear, 1967; Bushinski, 1964; Chauhan, 1979; Riggs, 1979a, 1979b). Apatite formation by non-replacement diagenesis of phosphates was, in turn, demonstrated in the Namibian shelf (Price and Calvert, 1978). Gel-like phosphates undergo at least a partial recrystallization during early diagenesis (Baturin and Dubinchuk, 1974a, 1974b) which causes the XRD characteristics of phosphates that remain not covered with bottom sediment to be typical of apatite, especially the carbonate fluorapatite (Dietz et al., 1942; Parker and Siesser, 1972; Parker, 1975; Birch, 1979a, 1979b; Mullins and Neumann, 1979). On the other hand, the present-day nature of several sea-floor phosphorites appears to be disputable (see e. g. Kolodny and Kaplan, 1970; Baturin et al., 1972; Burnett and Gomberg, 1977; Burnett and Veeh, 1977).

Gel-like materials obviously are soft and plastic. Baturin (1969) demonstrated a gradual hardening of initially soft phosphatic pellets from the South and West African shelf. Furthermore, Veeh et al. (1974) demonstrated with use of radiometric methods that unquestionable recent phosphorites are the only soft ones. The initial plasticity of the investigated phosphate pizolite structures from the high-tatric Albian limestones is suggested by the occurrence of load and intralaminar deformations. Furthermore, the observed stages of recrystallization resamble very closely those recorded by Baturin and Dubinchuk (1974a, 1974b) and Ilin et al. (1975), which corroborates the conclusion that the apatite found in the investigated pizolites is entirely diagenetic in origin.

The origin of microglobular structure of the investigated phosphate pizolites can hardly be explained with certainty because of considerable diagenetic effects. As evidenced by the nature of the contact of the microglobules with the phosphatic matrix, all the microglobules are primary structures. Some pre-diagenetic relics indicate the proportion of organic matter having been higher in the microglobules than in the matrix. Similar microstructures were described from the phosphatic ooids of the Phosphoria Formation and interpreted as initially soft and gel-like (Lowell, 1952). Baturin and Dubinchuk (1974b) illustrated phosphate microglobules from the sea-floor phosphorites of the Agulhas Bank. Moreover, microglobules that underwent a fibrous recrystallization of apatite were discovered by Ilin et al. (1975) in the phosphorites of the Kara Tau range. The origin of all those microglobules, however, remains thus far unclear. One may suppose that they developed from small accumulations of organic matter enriched in colloidal phosphates, stabilized at the surface of growing pizolite structures. The mode of recrystallization is indicative of variable distribution of organic matter in the microglobules. Activation of the center of a microglobule, being the richest in organic matter or even composed exclusively of it, resulted in development of geochemical conditions favourable for apatite crystallization. Such phosphatic microglobules enriched in organic matter were,

indeed, regarded as coccolite-like algal forms (Chauhan, 1979) or bacteria-like rods (Riggs, 1979a). Taken for granted that the microglobules are traces after some unicellular microorganisms, their systematic position cannot nevertheless be recognized because of diagenetic effects. The methods applied in the present study can hardly permit even a recognition of their eu- or prokaryotic organization (Golubić and Barghoorn, 1977, and references therein). On the other hand, some bacteria may contribute to precipitation of phosphates from sea-water (Malone and Towe, 1970). One may nevertheless claim that the considered microstructures can be more plausibly explained by accumulation of microorganisms, like that proposed by Kaźmierczak (1979), than by physiochemical activities in situ of microorganisms contributing to development of phosphatic pizolites.

Only these parts of the investigated pizolites which are poor in organic matter (light-yellow collophane) are partly recrystallized into microcrystalline apatite, whereas those rich in organic matter (dark-grey collophane) do never show any recrystallization discernible under TLM. Diagenetic formation of carbonate fluor-apatite under conditions of organic — matter decay commonly is observed in modern environments (Dietz et al., 1942; Baturin, 1969; Burnett, 1977; Price and Calvert, 1978). It was proposed also for various fossil phosphorites (Lowell, 1952; Patton and Matzko, 1959; Gulbrandsen, 1960; Bushinski, 1966). One may claim that recrystallization of massive and ultramicrocrystalline phosphates observed both in the microglobules and in the matrix in the investigated pizolite structures is to be attributed to diagenetic activation of the associated organic matter.

The phosphate pizolite structures from the high-tatric Albian limestones include variable amounts of non-detritic carbonates. The carbonate enclaves are discordant with the primary microstructures and therefore they are to be regarded as an effect of calcification of the phosphates. The fluorite recorded sporadically in the pizolites probably originated by replacement of fluorapatite by calcite, according to the reaction presented by Cook (1970).

All the investigated phosphate pizolite structures from the Tatra Mts are associated with eroded hardground surfaces, which indicates their development under conditions of intraformational reworking. This reworking caused the spherical to hemispherical shape of the pizolite structures. Any flat microstructural equivalents of the pizolite structures have not been observed in the high-tatric Albian limestones. The accretional growth and the intraformational reworking must have produced a set of physical conditions permitting development of spherical to hemispherical structures only. In fact, an alternation of phosphate formation and reworking commonly is claimed to be characteristic of phosphogenic open-shelf environments (Emery, 1960; Altschuler, 1965; Bromley,

1965 in: Bromley, 1967 and Bathurst, 1975; Kennedy and Garrison, 1975a, 1975b; Burnett and Gomberg, 1977; Birch, 1979c). The growth rate of the investigated pizolite structures can hardly be precisely determinated. The small thickness of the high-tatric Albian limestones, common occurrence of hardgrounds, and the mixed ammonite faunas indicative of 3 successive biostratigraphic zones (cf. Passendorfer, 1930) are strongly suggestive of very slow and commonly interrupted sedimentation. By itself, this is not to imply a slow growth of the phosphate pizolites but the latter occur exclusively in association with hardgrounds. On the other hand, non-deposition is a typical environment characteristic of various phosphorites found in open shelves and seamounts (see e. g. Dietz et al., 1942 as reinterpreted in: Emery, 1960; Hamilton and Rex, 1959; d'Anglejan, 1967; Marlowe, 1971; Anglada et al., 1975). One may therefore conclude that the phosphate pizolite structures from the high-tatric Albian limestones most probably originated owing to a slow accretional growth and intraformational reworking under conditions of periodically reworked hardground.

ACKNOWLEDGMENTS

My thanks are due to K. Ilska, A. Hoffman, T. M. Peryt, T. Piątkowski, and K. Radlicz for their help in the course of present study.

REFERENCES — WYKAZ LITERATURY

Altschuler Z. S. (1965), Precipitation and recycling of phosphate in the Florida land-pebble phosphate deposits. *U. S. Geol. Surv. Prof. Paper*, 525-B: B91—B95.

Anglada R., Froget C. and Récy J. (1975), Sédimentation valentie de diagenèse sous-marine su SE de la Nouvelle-Calédonie (dolomitisation, ferruginisation, phosphatisation). Sediment. Geol., 14 (4): 301—317.

Bathurst R. G. C. (1975), Carbonate Sediments and Their Diagenesis. *Developments in Sedimentology*, 12. Elsevier. Amsterdam. 632p.

Baturin G. N. (1969). Autigennyie fosforitovyie concrecii v sovremiennyh osadkah shelfa Iugo-Zapadnoi Afriki. *Dokl. Akad. Nauk SSSR*, 189 (6): 1359—1362.

Baturin G. N., Merkulova K. I. and Chalov P. I. (1972), Radiometric evidence for recent formation of phosphatic nodules in marine shelf sediments. *Mar. Geol.*, 13 (3): M37—M41.

Baturin G. N. and Dubinchuk V. T. (1974a). Electronno-microscopicheskoie issledovanie okeanskyh fosforitov. *Dokl. Akad. Nauk SSSR*, 218 (6): 1446—1449.

Baturin G. N. and Dubinchuk V. T. (1974b), Microstructures of Agulhas Bank phosphorites. *Mar. Geol.*, 16 (4): M63—M70.

Berge J. W. (1972), Discussion: Physical and chemical factors in the formation of marine apatite. *Econ. Geol.*, 67 (6): 824—827.

Birch G. F. (1979a), The nature and origin of mixed apatite/glauconite pellets from the continental shelf off South Africa. *Mar. Geol.*, 29 (1/4): 313—334.

Birch G. F (1979b), Phosphorite pellets and rock from the western continental margin and adjacent coastal terrace of South Africa. *Mar. Geol.*, 33 (1/2): 91—116.

Birch G. F. (1979c), Phosphatic rock on the western margin of South Africa. *Jour Sediment. Petrol.*, 49 (1): 93—110.

Borza K. and Martiny E. (1962), Výskum glaukonitového vápence albu Javorovej doliny v Tatrách. *Geol. Sb.*, 13 (1): 161—170.

Bromley R. G. (1967), Marine phosphorites as depth indicators. *Mar. Geol.*, 5 (5/6): 503—509.

Burnett W. C. (1977), Geochemistry and origin of phosphorite from off Peru and Chile. *Geol. Soc. Amer. Bull.*, 88 (6): 813—823.

Burnett W. C. and Gomberg D. N. (1977), Uranium oxidation and probable subaerial weathering of phosphatized limestone from the Pourtales Terrace. *Sedimentology*, 24 (2): 291—302.

Burnett W. C. and Veeh H. H. (1977), Uranium-series disequilibrium studies in phosphorite nodules from the west coast of South America. *Geochim. Cosmochim. Acta*, 41 (6): 755—764.

Bushinski G. I. (1966), Drevnyie Fosfority Azii i ih Genezis. *Izd. Nauka.* Moskva. 188p.

Chauhan D. S. (1979), Phosphate-bearing stromatolites of the Precambrian Aravalli phosphorite deposits of the Udaipur region, their environmental significance and genesis of phosphorite. *Precambrian Res.*, 8 (1/2): 95—126.

Cook P. J. (1970), Repeated diagenetic calcitization, phosphatization, and silification in the Phosphoria Formation. *Geol. Soc. Amer. Bull.* 81 (7): 2107—2116.

d'Anglejan B. F. (1967), Origin of marine phosphorites off Baja California, Mexico. *Mar. Geol.*, 5 (1): 15—44.

Dietz R. S., Emery K. O. and Shepard F. P. (1942), Phosphorite deposits on the sea floor off southern California. *Geol. Soc. Amer. Bull.*, 53 (6): 815—848.

Emery K. O. (1960), The Sea off Southern California. John Wiley and Sons, Inc. New York. 366p.

Fuller A. O. (1979), Phosphate occurrence on the western and southern coastal areas and continental shelves of southern Africa. *Econ. Geol.*, 74 (2): 221—231.

Golubić S. and Barghoorn E. S. (1977), Interpretation of microbial fossils with special reference to the Precambrian. in: E. Flügel (Ed.) Fossil Algae. Springer-Verlag. Berlin. p. 1—14.

Gulbrandsen R. A. (1960), Petrology of the Meadle Peak phosphatic shale member of the Phosphoria Formation at Coal Canyon, Wyoming. *U. S. Geol. Surv. Bull.*, 1111-C: 71—144.

Gulbrandsen R. A. (1969), Physical and chemical factors in the formation of marine apatite. *Econ. Geol.*, 64 (4): 365—382.

Gulbrandsen R. A. (1970), Relation of carbon dioxide content of apatite of the Phosphoria Formation to regional facies. *U. S. Geol. Surv. Prof. Paper*, 700-B: B9—B13.

Hamilton E. L. and Rex R. W. (1959), Lower Eocene phosphatized *Globigerina* ooze from Sylvenia Guyot. *U. S. Geol. Surv. Prof. Paper*, 260-W: 785—795.

Ilin A. W, Ratnikova G. I. and Sergeeva N. E. (1975), O petrograficheskyh tipah plastovyh fosforitov i ih microstrukturie. *Litol. Polezn. Iskop.*, 1: 108—119.

Kaźmierczak J. (1979), The eukaryotic nature of *Eosphaera*-like ferriferous structures from the Precambrian Gunflint Iron Formation, Canada: a comparative study. *Precambrian Res.*, 9 (1/2): 1—22.

Kennedy W. J. and Garrison R. E. (1975a), Morphology and genesis of hardgrounds and nodular chalks in the Upper Cretaceous of southern England. *Sedimentology*, 22 (3): 311—386.

Kennedy W. J. and Garrison R. E. (1975b), Morphology and genesis of nodular phosphates in the Cenomanian Glauconitic Marl of south-east England. *Lethaia*, 8 (4): 339—360.

Kolodny Y. and Kaplan I. R. (1970), Uranium isotopes in sea-floor phosphorites. *Geochim. Cosmochim. Acta*, 34 (1): 3—24.

Kotański Z. (1961), Tektogeneza i rekonstrukcja paleogeografii pasma wierchowego w Tatrach. Tectogénèse et reconstitution de la paléogéographie de la zone haut-tatrique dans les Tatras. *Acta Geol. Polon.*, 11 (2/3): 187—412.

Kušik R. (1959), Litologia sedimentarnych serii uzemia Oravic. *Geol. Sb.*, 10 (1): 203—222.

Lefeld J. (1968), Stratygrafia i paleogeografia dolnej kredy wierchowej Tatr. Stratigraphy and palaeogeography of the high-tatric Lower Cretaceous in the Tatra Mountains. *Studia Geol. Polon.*, 24: 1—115.

Lowell W. R. (1952), Phosphatic rocks in the Deer Creek-Wells Canyon area, Idaho. *U. S. Geol. Surv. Bull.*, 982-A, 51p.

Malone Ph. G. and Towe K. M. (1970), Microbial carbonate and phosphate precipitates from sea water cultures. *Mar. Geol.*, 9 (5): 301—309.

Marlowe J. I. (1971), Dolomite, phosphorite, and carbonate diagenesis on a Caribbean seamount. *Jour. Sediment. Petrol.*, 41 (3): 803—827.

McConnell D. (1965), Precipitation of phosphates in sea water. *Econ. Geol.*, 60 (5): 1059—1062.

McConnell D. (1973), Apatite, its Crystal Chemistry, Mineralogy, Utilization, and Geologic and Biologic Occurrences. Applied Mineralogy, 5. Springer-Verlag. Wien. 103p.

Mullins H. T. and Neumann A. C. (1979), Geology of the Miami Terrace and its paleo-oceanographic implications. *Mar. Geol.*, 30 (3/4): 205—232.

Nathan Y. and Lucas J. (1976), Expériences sur la précipitation directe de l'apatite dans l'eau de mer: implication dans la genèse des phosphorites. *Chem. Geol.*, 18 (3): 181—186.

Niegodzisz J. (1965), Stromatolity z albu wierchowego Tatr. Stromatolites from the high-tatric Albian of the Tatra Mountains. *Acta Geol. Polon.*, 15 (4): 529—549.

Parker R. J. (1975), The petrology and origin of some glauconitic and glauco-conglomeratic phosphorites from the South African continental margin. *Jour. Sediment. Petrol.*, 45 (1): 230—242.

Parker R. J. and Siesser W. G. (1972), Petrology and origin of some phosphorites from the South African continental margin. *Jour. Sediment. Petrol.*, 42 (2): 434—440.

Passendorfer E. (1921), Kreda serii wierchowej w Tatrach. Sur la Crétacé hauttatrique de la Tatra. *Spraw. Państw. Inst. Geol.*, 1 (2/3): 217—250.

Passendorfer E. (1930), Étude stratigraphique et paléontologique du Crétacé de la série hauttatrique dans les Tatras. *Prace Państw. Inst. Geol.*, 2 (4): 511—676.

Patton W. W. and Matzko J. J. (1959), Phosphate deposits in northern Alaska. *U. S. Geol. Surv. Prof. Paper*, 302-A, 16p.

Pevear D. R. (1967), Shallow water phosphorites. *Econ. Geol.*, 62 (4): 562—575.
Price N. B. and Calvert S. E. (1978), The geochemistry of phosphorites from the Namibian shelf. *Chem. Geol.*, 23 (2): 151—170.
Riggs S. R. (1979a), Petrology of the Tertiary phosphorite system of Florida. *Econ. Geol.*, 74 (2): 195—220.
Riggs S. R. (1979b), Phosphorite sedimentation in Florida — A model phosphogenic system. *Econ. Geol.*, 74 (2): 285—314.
Turnau-Morawska M. (1960), Wapień glaukonitowy z albu Wielkiej Równi w Tatrach. Albian glauconitic limestone of Wielka Równień in the Tatra Mts. *Acta Geol. Polon.*, 10 (3): 265—281.
Veeh H. H., Calvert S. E. and Price N. B. (1974), Accumulation of uranium in sediments and phosphorites on the south west African shelf. *Mar. Chem.*, 2: 189—202.
Veeh H. H. and Burnett W. C. (1978), Uranium-series dating of insular phosphorite from Ebon atoll, Micronesia. *Nature*, 274 (5670): 460—462.

EXPLANATIONS TO PLATES — OBJAŚNIENIA PLANSZ

Plate 1 — Plansza 1

Fig. 1. Phosphate-pizolitic lamination; TLM, nicols parallel; bar equals 500 μm. Note the interlaminar boundaries accentuated with films of iron oxides (black), or an increased proportion of organic matter (grey), or textural changes in collophane.

Fig. 1. Fosforanowa laminacja pizolitowa; mikroskop polaryzacyjny, nikole równoległe; skala odpowiada 500 μm. Granice pomiędzy laminami podkreślone filmami tlenków żelaza (czarne barwy), zwiększoną zawartością materii organicznej (szare barwy), lub teksturalnymi zmianami kollofanu.

Fig. 2. Lenses of non-phosphatic detritic material within pizolitic lamination; TLM, nicols parallel; bar equals 1 mm. Arrowed are areas enlarged in pl 4, figs. 1—2.

Fig. 2. Soczewki niefosforanowego materiału detrytycznego w obrębie laminacji pizolitowej; mikroskop polaryzacyjny, nikole równoległe; skala odpowiada 1 mm. Strzałkami zaznaczono miejsca powiększone na pl. 4, figs. 1—2.

Plate 2 — Plansza 2

Fig. 1. Microglobular structure of phosphate pizolites; TLM, nicols parallel; bar equals 100 μm. Note that the microglobules are richer in organic matter (black to dark-grey) than the microlaminated collophane matrix (grey).

Fig. 1. Struktura mikroglobularna fosforanowych pizolitów; mikroskop polaryzacyjny, nikole równoległe; skala odpowiada 100 μm. Mikroglobule silniej wzbogacone w materię organiczną (czarne i ciemnoszare barwy) niż mikrolaminowany kollofanowy cement (szare barwy).

Fig. 2. Enlarged fragment of the same figure; TLM, nicols parallel; bar equals 25 μm. Note contacts of the microglobules and the microlaminated matrix, and variable stages of activation of the organic matter contained by the

microglobules. Arrowed are examples of plastic deformations of the microglobules.

Fig. 2. Powiększony fragment powyższej figury; mikroskop polaryzacyjny, nikole równoległe; skala odpowiada 25 μm. Widoczne kontakty mikroglobul z mikrolaminowanym cementem oraz różne stadia uruchamiania materii organicznej w mikroglobulach. Strzałkami zaznaczono przykłady plastycznych odkształceń mikroglobul.

Plate 3 — Plansza 3

Fig. 1. Uneven accretional surface of a phosphate-pizolitic lamina; SEM; bar equals 100 μm.

Fig. 1. Nierówna akrecyjna powierzchnia fosforanowej laminy pizolitowej; mikroskop skaningowy; skala odpowiada 100 μm.

Fig. 2. Enlarged fragment of the same figure; SEM; bar equals 10 μm. Note the recrystallization into ultra- and microcrystalline phosphate aggregates.

Fig. 2. Powiększony fragment figury 1; mikroskop skaningowy; skala odpowiada 10 μm. Widoczna agregatowa rekrystalizacja do ultra- i mikrokrystalicznych fosforanów.

Fig. 3. Microglobular structure of the surface of a phosphate-pizolitic lamina; SEM; bar equals 100 μm.

Fig. 3. Powierzchnia fosforanowej laminy pizolitowej wykazująca strukturę mikroglobularną; mikroskop skaningowy; skala odpowiada 100 μm.

Fig. 4. Vertical section through a phosphate-pizolitic lamina microglobular in structure; SEM; bar equals 50 μm.

Fig. 4. Przekrój prostopadły przez fosforanową laminę pizolitową wykazującą strukturę mikroglobularną; mikroskop skaningowy; skala odpowiada 50 μm.

Fig. 5. Microglobule with recrystallized phosphate aggregates in the center; SEM; bar equals 2 μm. Note the margins of the microglobule contacting with the massive to ultramicrocrystalline matrix.

Fig. 5. Mikroglobula z widoczną w centrum agregatową rekrystalizacją fosforanów; mikroskop skaningowy; skala odpowiada 2 μm. Brzegi mikroglobuli zlane z masywnym i ultramikrokrystalicznym cementem.

Fig. 6. Recrystallized microglobule; SEM; bar equals 5 μm. Note the ultramicrocrystalline phosphate aggregates and the considerable porosity effected by activation of organic matter.

Fig. 6. Rekrystalizacja mikroglobuli; mikroskop skaningowy; skala odpowiada 5 μm. Widoczne ultramikrokrystaliczne agregaty fosforanów; duża porowatość wynika z uruchomienia materii organicznej.

Plate 4 — Plansza 4

Figs. 1, 2. Load deformations of collophane microlaminae underlying calcisphaeres filled up with microsparite; enlarged fragments of pl. 1, fig. 2; TLM, nicols parallel; bar equals 100 μm.

Fig. 1, 2. Plastyczne obciążeniowe deformacje mikrolamin kollofanowych poniżej kontaktów z kalcisferami wypełnionymi mikrosparytem; powiększone fragmenty z pl. 1, fig. 2; mikroskop polaryzacyjny, nikole równoległe; skala odpowiada 100 μm.

Fig. 3. Clacisphaere filled up with massive phosphates partly recrystallized into ultra- and microcrystalline phoshate aggregates; SEM; bar equals 10 μm.
Fig. 3. Kalcisfera wypełniona masywnymi fosforanami, częściowo zrekrystalizowanymi do agregatów ultra- i mikrokrystalicznych fosforanów; mikroskop skaningowy; skala odpowiada 10 μm.
Fig. 4. Chamber of planktic foram filled up with partly recrystallized massive phosphates; SEM; bar equals 20 μm. Note that the nature of the fill is suggestive of its development from the margins of the chamber inwards.
Fig. 4. Komora planktonicznej otwornicy wypełniona częściowo zrekrystalizowanymi masywnymi fosforanami; mikroskop skaningowy; skala odpowiada 20 μm. Charakter wypełnienia wskazuje na przyrost fosforanów od brzegów do centrum komory.

Plate 5 — Plansza 5

Fig. 1. Recrystallization of collophane into microcrystalline apatite; TLM; nicols almost crossed; bar equals 50 μm. Arrowed is a recrystallized microlamina (light) and its contact with non-recrystallized microglobules (dark-grey).
Fig. 1. Rekrystalizacja kollofanu do mikrokrystalicznego apatytu; mikroskop polaryzacyjny, nikole prawie skrzyżowane; skala odpowiada 50 μm. Strzałka wskazuje zrekrystalizowaną mikrolaminę (jasne barwy) i jej kontakt z mikroglobulami nie wykazującymi rekrystalizacji (ciemnoszare barwy).
Fig. 2. Relics of microglobules rich in organic matter (black to dark-grey) within recrystallized microcrystalline matrix (light); TLM, nicols almost crossed; bar equals 50 μm.
Fig. 2. Relikty wzbogaconych w materię organiczną mikroglobul (czarne i ciemnoszare barwy) w zrekrystalizowanym mikrokrystalicznym tle (jasne barwy); mikroskop polaryzacyjny, nikole prawie skrzyżowane; skala odpowiada 50 μm.
Fig. 3. Massive phosphates recrystallized into ultramicrocrystalline aggregates; SEM; bar equals 5 μm.
Fig. 3. Rekrystalizacja masywnych do ultramikrokrystalicznych agregatowych fosforanów; mikroskop skaningowy; skala odpowiada 5 μm.
Fig. 4. Massive phosphates recrystallized into ultramicrocrystalline aggregates; SEM; bar equals 5 μm. Note the porosity of the phosphate aggregates effected by activation of organic matter.
Fig. 4. Rekrystalizacja masywnych do ultramikrokrystalicznych agregatowych fosforanów; mikroskop skaningowy; skala odpowiada 5 μm. Widoczna znaczna porowatość agregatowych fosforanów spowodowana uruchomieniem materii organicznej.

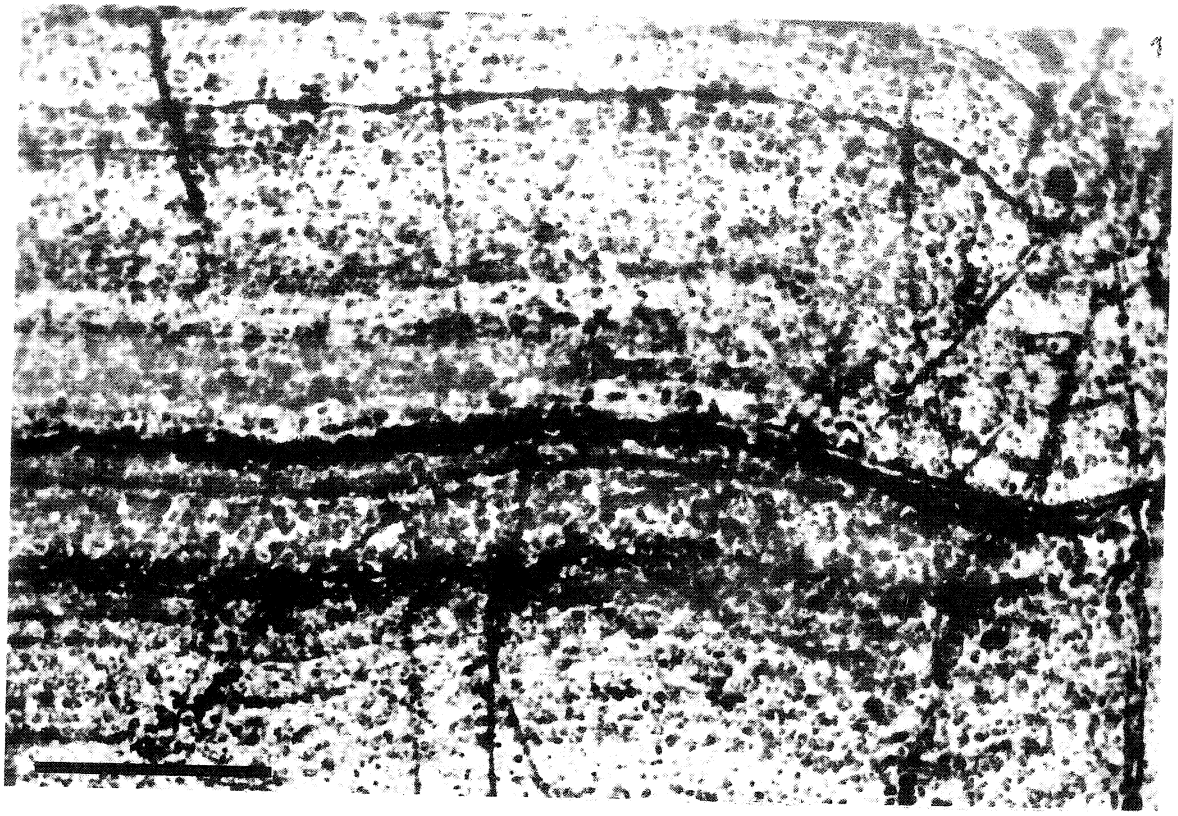

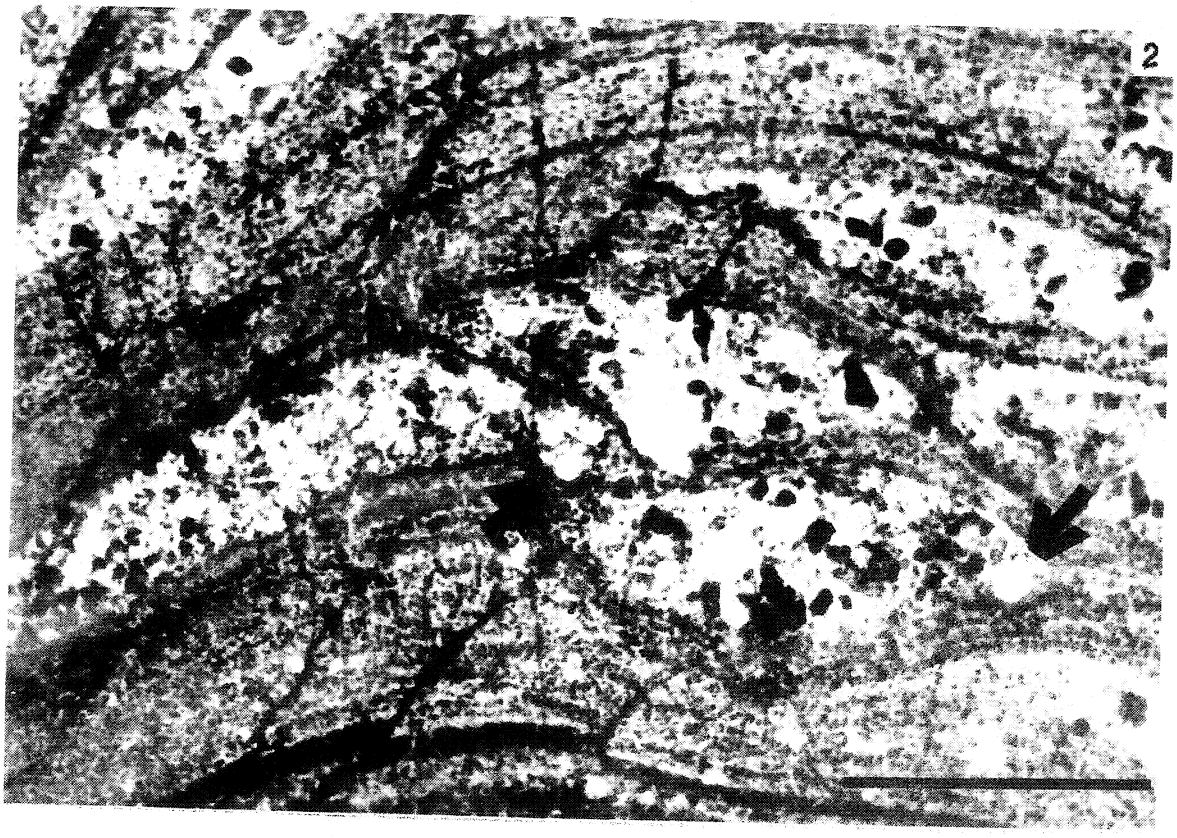

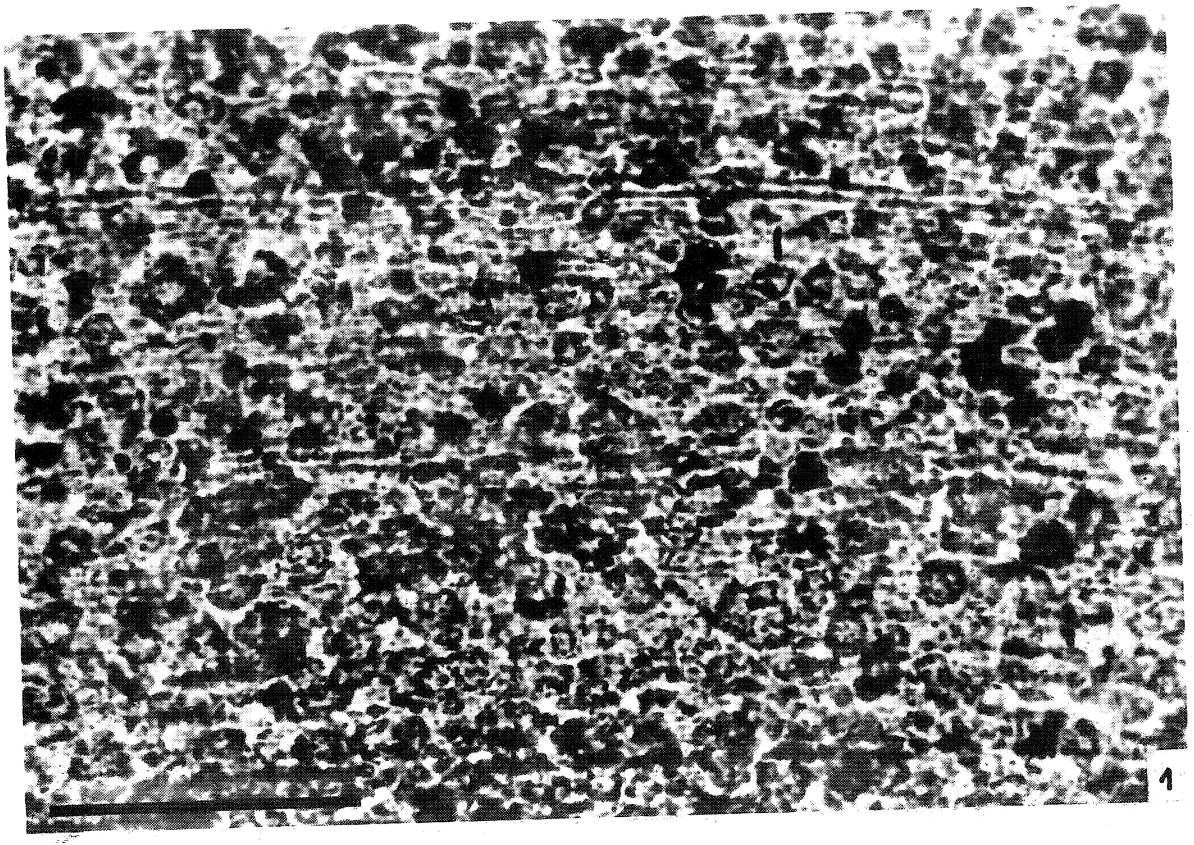

1

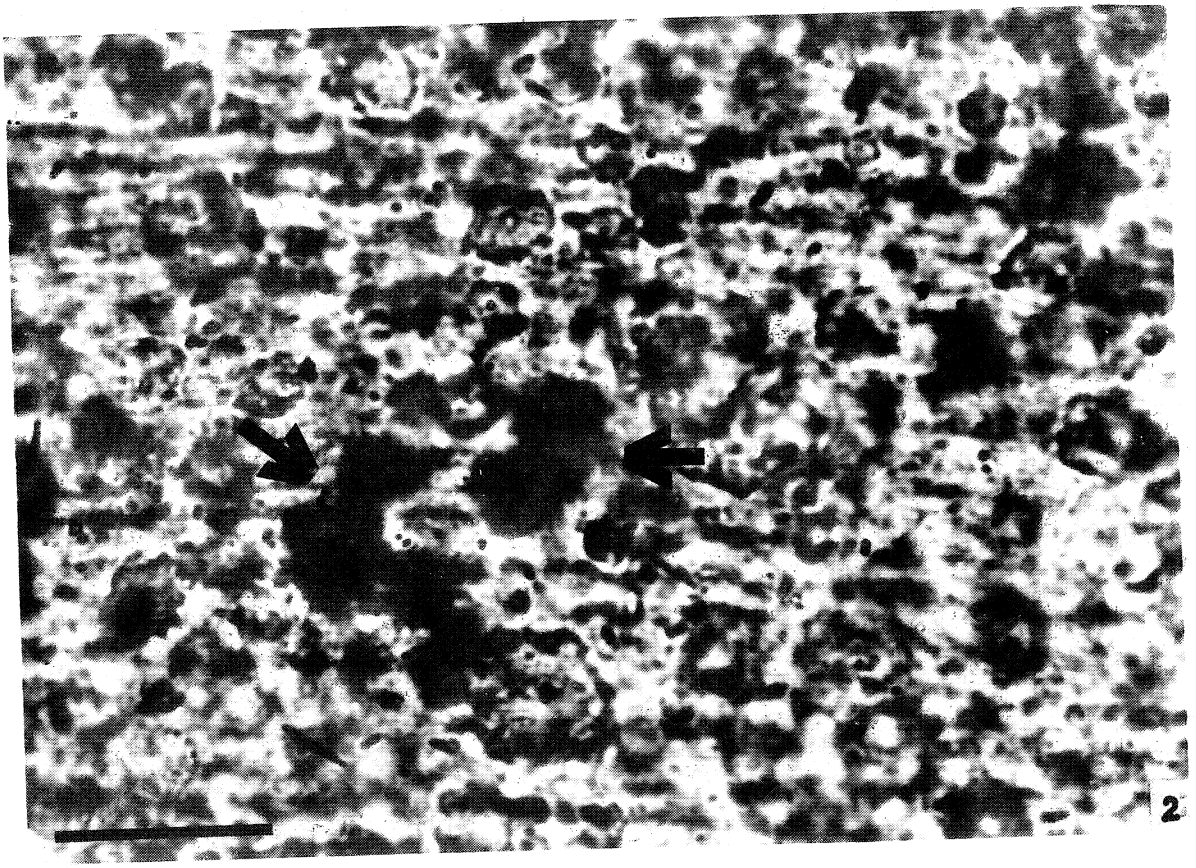

2

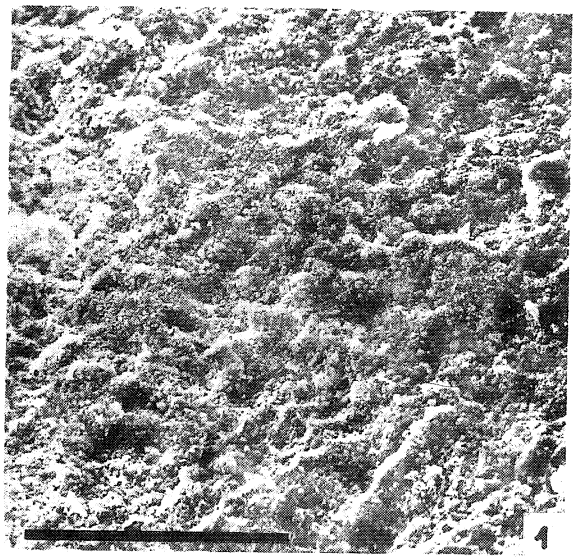
1

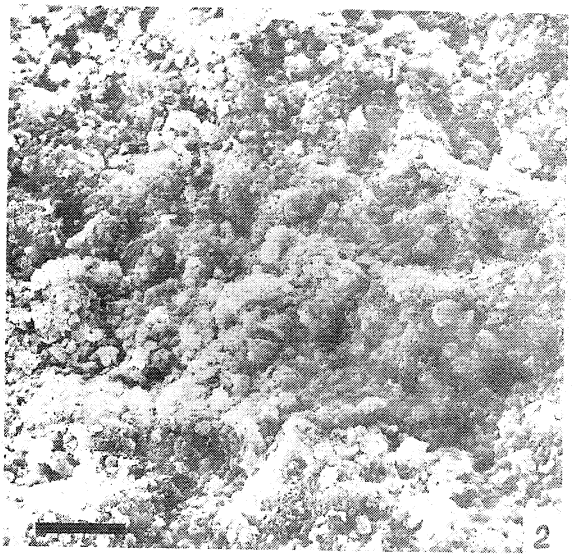
2

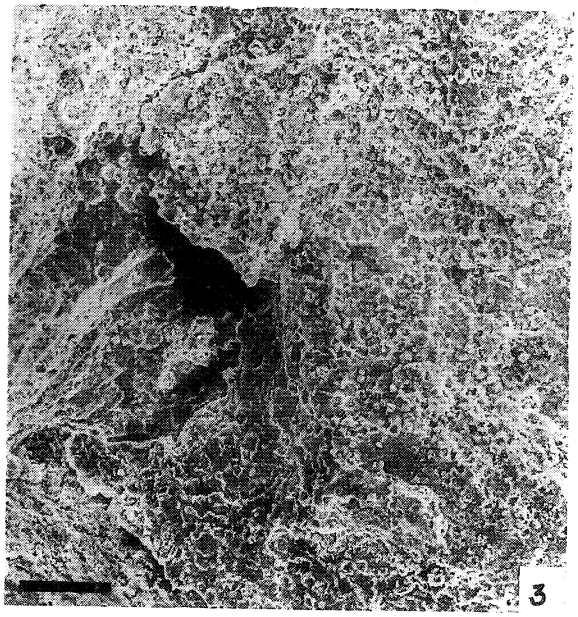
3

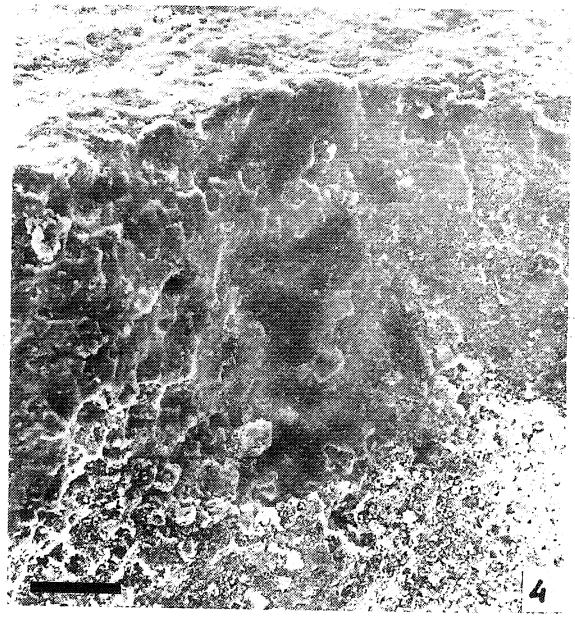
4

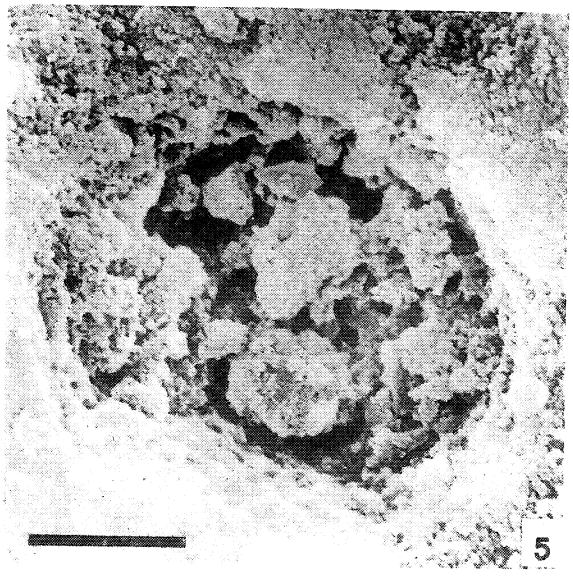
5

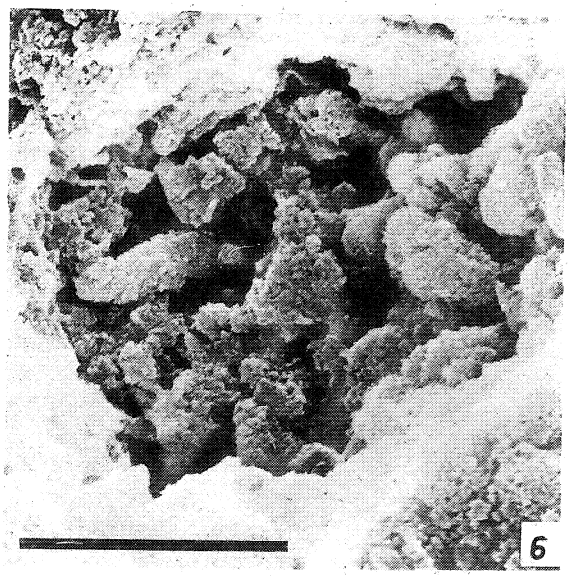
6

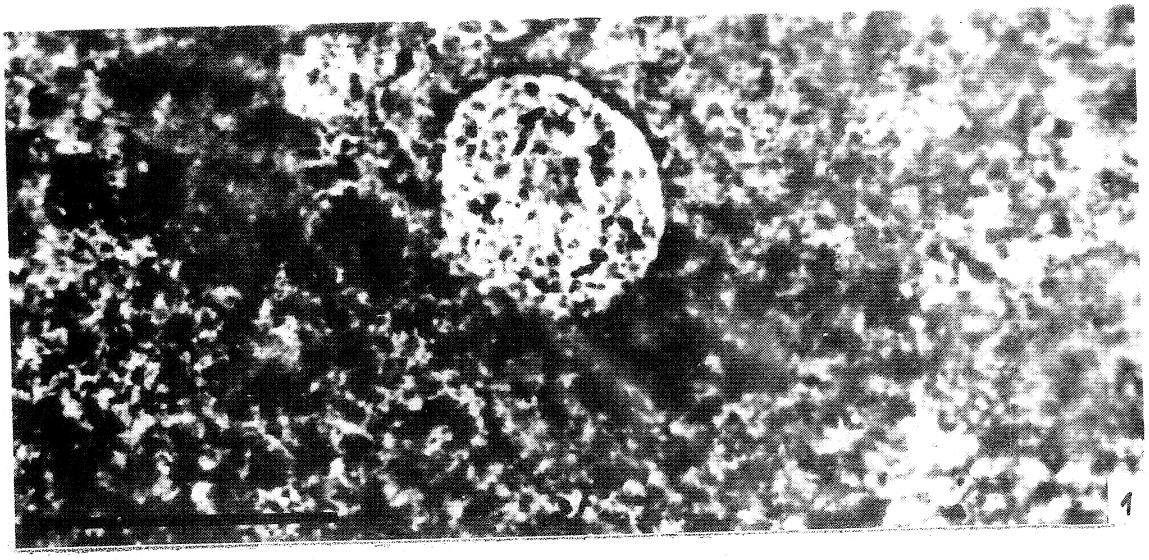

1

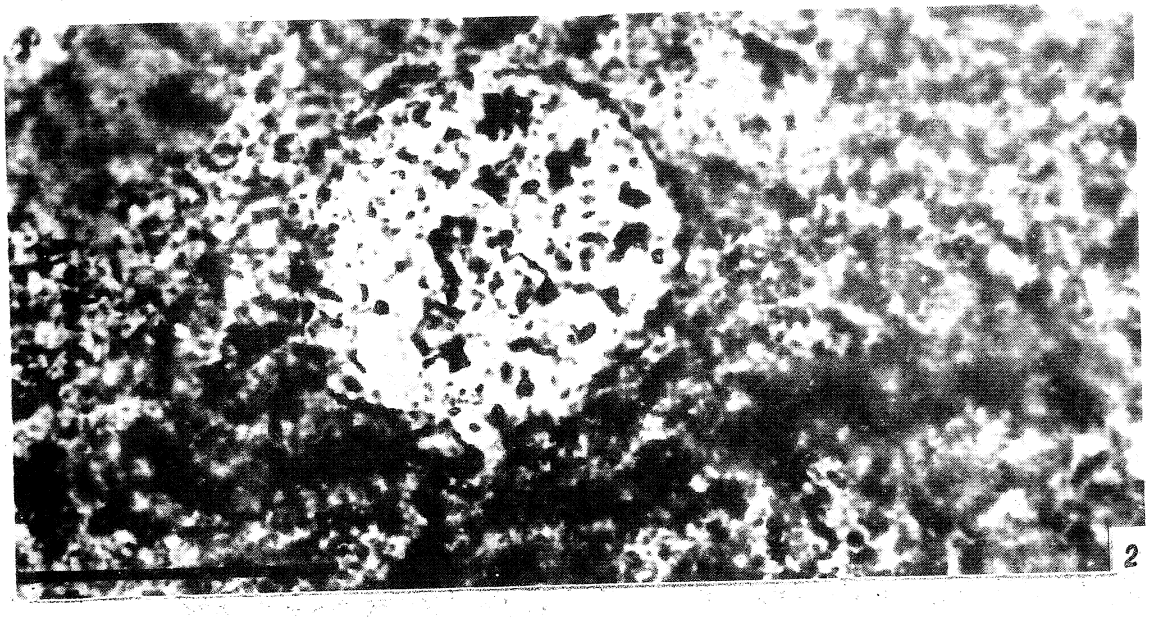

2

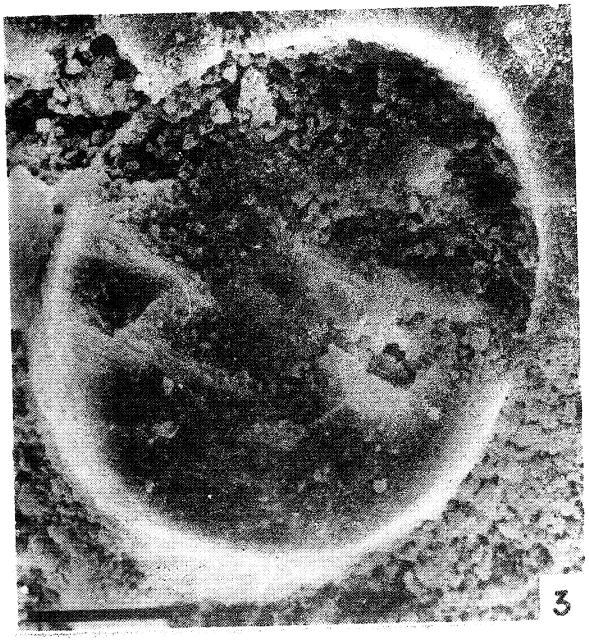

3

4

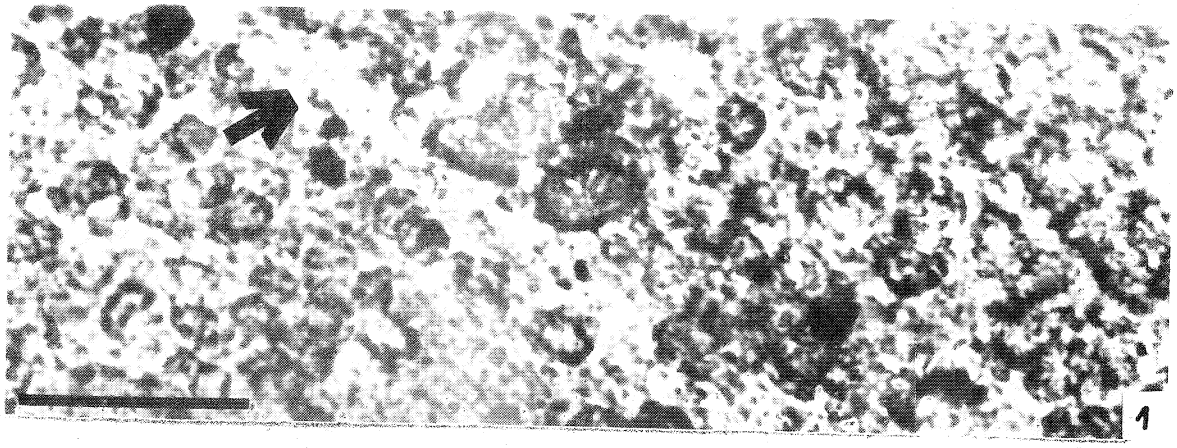

1

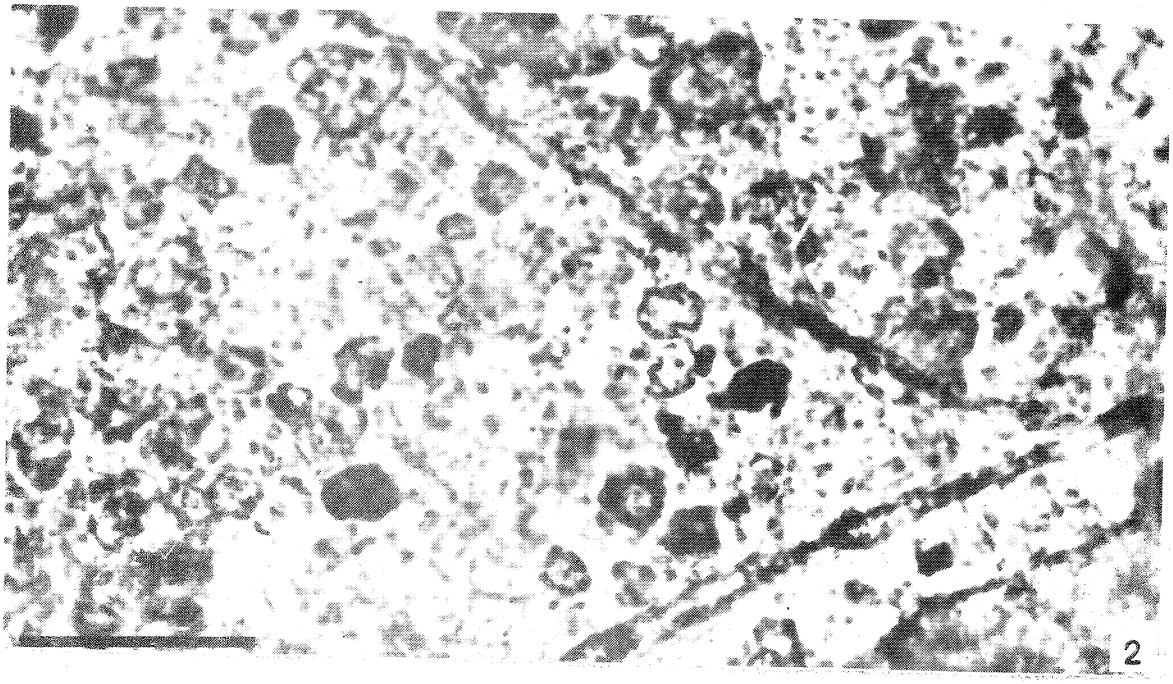

2

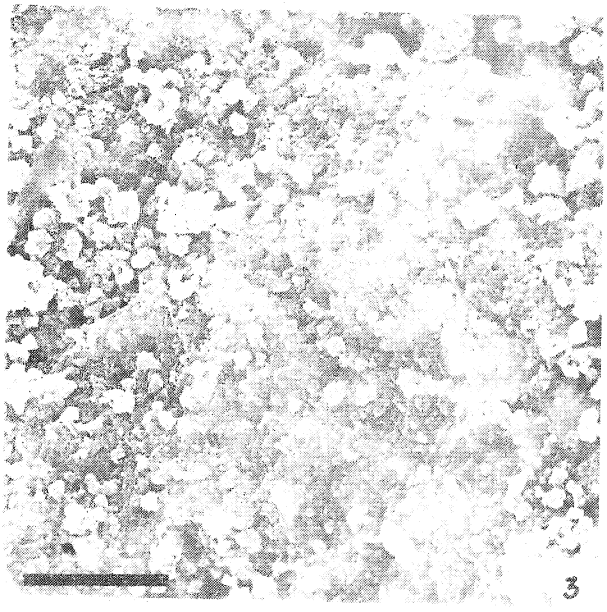

3

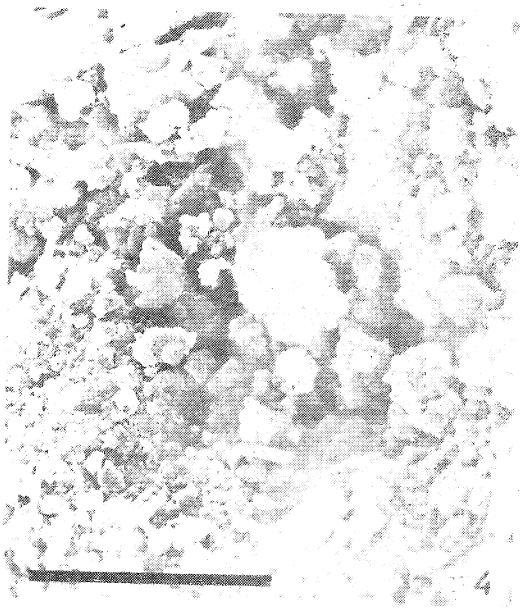

4